Acta Crystallographica Section F
Structural Biology and Crystallization Communications
ISSN 1744-3091

Structure of a mutant β toxin from *Staphylococcus aureus* reveals domain swapping and conformational flexibility

Andrew C. Kruse,‡ Medora J. Huseby,§ Ke Shi, Jeff Digre, Douglas H. Ohlendorf and Cathleen A. Earhart*

Department of Biochemistry, Molecular Biology and Biophysics, University of Minnesota, Minneapolis, MN 55455, USA

‡ Current address: Department of Molecular and Cellular Physiology and Medicine, Stanford University, Stanford, California, USA.
§ Current address: Departments of Medicine and Microbiology and Immunology, University of California at San Francisco, San Francisco, California, USA.

Correspondence e-mail: earhart@umn.edu

Received 12 October 2010
Accepted 11 February 2011

PDB Reference: mutant β toxin from *Staphylococcus aureus*, 3k55.

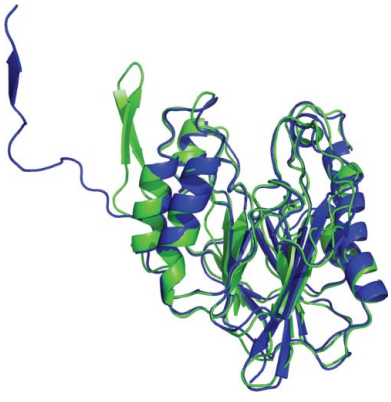

The 3.35 Å resolution crystal structure of a mutant form of the staphylococcal sphingomyelinase β toxin in which a conserved hydrophobic β-hairpin has been deleted is reported. It is shown that this mutation induces domain swapping of a C-terminal β-strand, leading to the formation of dimers linked by a conformationally flexible hinge region. Eight dimers are seen in the asymmetric unit, exhibiting a broad spectrum of conformations trapped in place by intermolecular contacts within the crystal lattice. Furthermore, the 16 monomers within each asymmetric unit exhibit a remarkable heterogeneity in thermal factors, which can be accounted for by the varying degrees to which each monomer interacts with other molecules in the crystal. This structure provides a unique example of the challenges associated with crystallographic study of flexible proteins.

1. Introduction

β Toxin is a class C neutral sphingomyelinase secreted by the pathogenic bacterium *Staphylococcus aureus*. It was originally identified from its hemolytic activity towards sheep erythrocytes and was subsquently shown to catalyze the hydrolysis of sphingomyelin to give ceramide and phosphocholine (Dinges *et al.*, 2000). We have previously demonstrated that β toxin kills proliferating human lymphocytes and that this toxicity is linked to its sphingomyelinase activity (Huseby *et al.*, 2007). Others have demonstrated its toxicity to monocytes (Walev *et al.*, 1996) and T cells (Collins *et al.*, 2008) and β toxin has also been shown to increase virulence in murine model systems, leading to enhanced bacterial proliferation in mammary-gland infections (Bramley *et al.*, 1989) and neutrophil-mediated lung injury (Hayashida *et al.*, 2009).

Like sphingomyelinases from *Bacillus cereus* (Ago *et al.*, 2006) and *Listeria ivanovii* (Openshaw *et al.*, 2005), wild-type β toxin folds into a four-layer sandwich comprised of two layers of antiparallel β-strands flanked by two layers of α-helices. This overall fold is shared by other phosphodiesterases, including mammalian DNase I (Oefner & Suck, 1986) and *Escherichia coli* exonuclease III (Mol *et al.*, 1995). Notably, β toxin and other bacterial neutral sphingomyelinases possess a hydrophobic β-hairpin which extends away from the protein, a feature that is not seen in nucleases such as DNase I. Openshaw and coworkers have proposed that this structure mediates localization of sphingomyelinases to host cell membranes, where enzymatic hydrolysis of sphingomyelin occurs (Openshaw *et al.*, 2005). Site-directed mutagenesis experiments by Ago and coworkers have offered support for this model (Ago *et al.*, 2006).

The role of the hydrophobic β-hairpin in biological toxicity and the *in vitro* sphingomyelinase activity of β toxin have been investigated by mutagenesis and detailed results of these experiments will be reported in the near future. This work involved the preparation and crystallographic characterization of several mutant forms of β toxin, including one in which the β-hairpin (comprised of residues 272–282) was deleted in its entirety. Here, we discuss the structure of this mutant, which reveals several unexpected features, including domain swapping of a C-terminal β-strand and the presence of a multitude of conformational states within a single crystal.

2. Materials and methods

2.1. Protein expression and purification

The gene for β toxin from *S. aureus* strain RN4220 (excluding the N-terminal signal sequence) was cloned into a pET28b vector with an N-terminal His_6 tag and with the codons for residues 272–282 deleted by cassette mutagenesis. The resulting vector was transformed into *Escherichia coli* strain BL21 (DE3) and cells were grown at 310 K with shaking to an optical density of 0.5 measured at λ = 600 nm. Protein expression was induced with 1 m*M* isopropyl β-D-1-thio-galactopyranoside. Cells were harvested 4 h later by centrifugation. Protein purification was performed as described elsewhere (Huseby *et al.*, 2007). Briefly, cells were lysed by sonication and centrifuged to remove cellular debris. β Toxin was purified from the resulting supernatant by Ni–NTA affinity chromatography and dialyzed into a buffer consisting of 0.1 *M* imidazole pH 8.0, 0.5 *M* NaCl, 1 m*M* β-mercaptoethanol and 1 m*M* EDTA. Prior to crystallization, purified protein was concentrated to 12 mg ml^{-1} with Centricon YM-10 centrifugal concentrator tubes (Amicon).

2.2. Crystallization

Initially, extensive screening of crystallization conditions failed to yield crystals suitable for structure determination, but conditions amenable to the formation of spherulites were found with Hampton Research Index Screen condition No. 77. Further screening around this condition led to the formation of diffraction-quality crystals. Crystals were grown by sitting-drop vapor diffusion of 2 µl protein solution mixed with 2 µl reservoir solution against 100 µl 0.1 *M* Tris–HCl pH 7.0–8.5, 26–32% polyethylene glycol 3350 and 0.2 *M* lithium sulfate, with the addition of 0.4 µl 0.1 *M* betaine hydrochloride to the crystallization drop.

Table 1
Data-collection and refinement statistics.

Values in parentheses are for the highest shell.

Space group	$P2_1$
Unit-cell parameters (Å, °)	a = 151.4, b = 134.5, c = 161.5, $\alpha = \gamma = 90$, $\beta = 119.9$
Resolution limits (Å)	32.6–3.35 (3.40–3.35)
Unique reflections	74076 (4320)
Completeness (%)	96.5 (72.8)
Multiplicity	2.6 (1.6)
$\langle I\rangle/\langle\sigma(I)\rangle$	11.2 (1.9)
R_{merge} (%)	8.8 (39.6)
R_{work}/R_{free} (%)	22.9/27.5
R.m.s.d. from ideal values	
Bonds (Å)	0.008
Angles (°)	1.333
Ramachandran plot	
Most favored regions (%)	83.9
Additionally allowed regions (%)	15.9
Generously allowed regions (%)	0.1
Forbidden regions (%)	0.0

2.3. Data collection and structure determination

Crystals were soaked in mother liquor with 20% glycerol as a cryoprotectant for 30 s prior to freezing in liquid nitrogen. Data collection was performed on beamline 14-BM-C at the Advanced

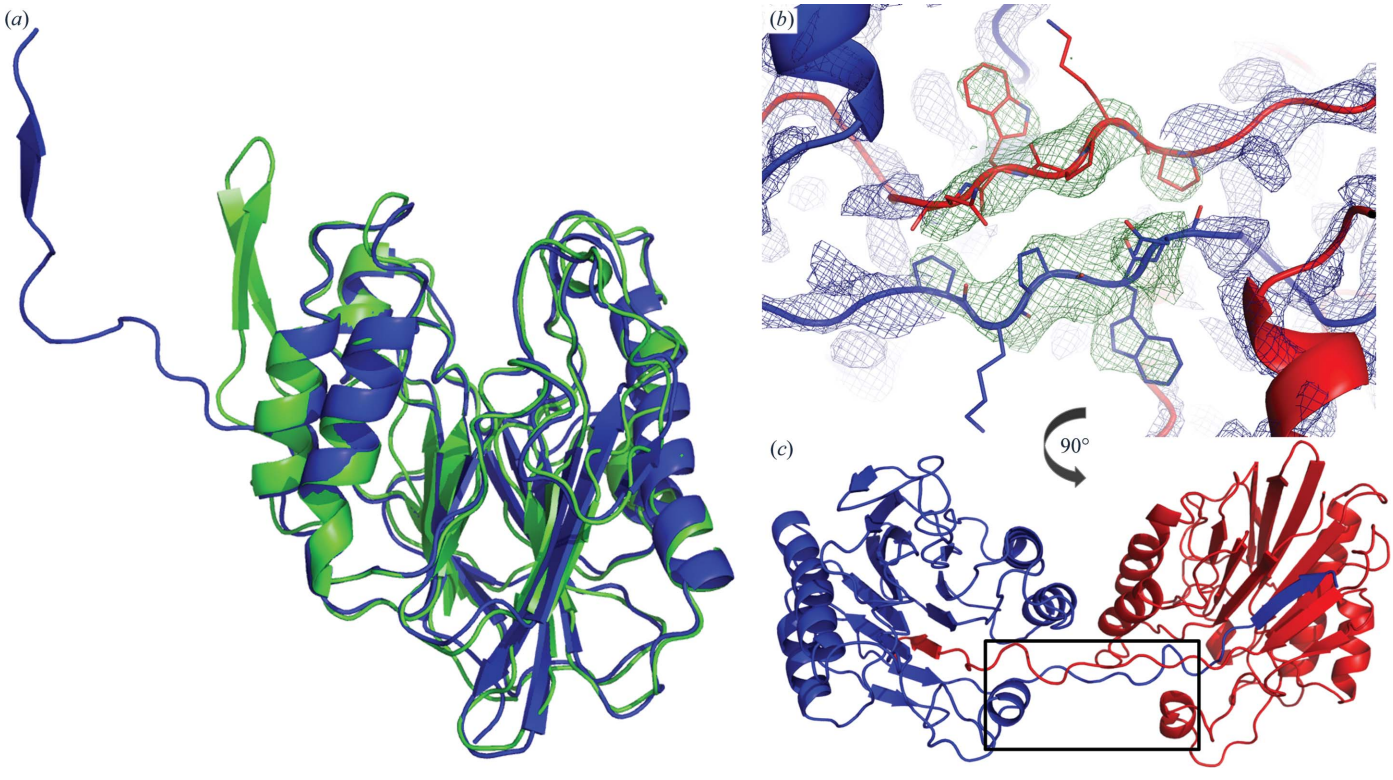

Figure 1
(*a*) Superimposition of the structures of wild-type β toxin (green) and β toxin in which the β-hairpin has been deleted (blue) shows little difference except for the β-hairpin region and the C-terminus of the mutant which is involved in domain-swapping interactions with another monomer (not shown). The C^{α} r.m.s.d. over residues 7–271 (that is, excluding the site of the mutation and the residues following it) is 0.71 Å. (*b*) Drawing of electron density at the domain-swap site (hinge region). Shown in green is a simulated-annealing OMIT map (delete residues 269–273 of each monomer) contoured at 2σ. A $2F_o - F_c$ electron-density map contoured at 1.5σ is shown in blue. The refined structures of residues 269–273 are shown as sticks. (*c*) Overall view of a single dimer showing domain swapping of the C-terminal β-strand. The orientation is rotated 90° around the horizontal axis relative to (*b*).

Photon Source, Argonne National Laboratory using an ADSC Quantum 315 detector. Data were processed with the *HKL*-2000 suite (HKL Research Inc.; Otwinowski & Minor, 1997). The structure was solved by molecular replacement using *Phaser* (McCoy, 2007) with the coordinates of F277A/P278A β toxin (PDB entry 3i48; M. Huseby, K. Shi, A. C. Kruse, J. Digre, F. Mengistu, G. A. Bohach, P. S. Schlievert, D. H. Ohlendorf & C. A. Earhart, unpublished work) as a search template. Even after optimizing the search parameters, an initial search with *Phaser* could identify only nine monomers, which was far fewer than the 15–20 expected from Matthews analysis (Matthews, 1968). This partial solution yielded a map that revealed density corresponding to several other monomers, which were placed by fitting the template monomer structure to the $F_o - F_c$ map with *MOLREP* (Vagin & Teplyakov, 1997). Iterating this procedure afforded a nearly complete solution with 15 monomers. Only at this point did density corresponding to the last monomer become visible. Following refinement it became apparent that this monomer has a significantly higher mean thermal factor than any other in the structure, accounting for the difficulty in locating it during molecular refinement. TLS refinement was performed using *PHENIX* (Adams *et al.*, 2002) with each monomer defined as a TLS group in accordance with the output from the *TLSMD* server (Painter & Merritt, 2006). Noncrystallographic symmetry restraints were applied during initial rounds of refinement by making poorly resolved monomers resemble those with lower thermal parameters (*B* factors). Manual rebuilding was performed with *Coot* (Emsley & Cowtan, 2004). Data-collection and refinement statistics are summarized in Table 1.

3. Results and discussion

3.1. Overall structure and domain swapping

Crystals of the mutant β toxin belonged to space group $P2_1$, with a large asymmetric unit containing 16 monomers (Table 1). The overall structure of the mutant is largely similar to that of wild-type β toxin (Fig. 1*a*), but following several refinement cycles it became apparent that the electron density at the site of the deletion could not be adequately modeled as a short loop as expected. Rather, density near the C-terminus forms a continuous path connecting each monomer to another (Fig. 1*b*), indicating swapping of the C-terminal strands between monomers (Fig. 1*c*). Each of the 16 monomers is paired with another at the site of the β-hairpin deletion and shows the same domain-swapping interaction. Thus, eight distinct dimers are present in the asymmetric unit, each held together by two chains running antiparallel to one another. Such β-strand domain-swapping interactions have been proposed to play a role in amyloidogenesis (Sambashivan *et al.*, 2005), although the mechanistic details that underlie this process remain elusive. Notably, the sequence of the swapped strand is highly conserved among sphingomyelinases as it contains active-site residues that are critical for enzymatic activity. The sphingomyelinase activity of the mutant measured in the manner described previously (Huseby *et al.*, 2007) was only slightly reduced compared with that of the wild type, indicating that the domain swapping does not significantly impede catalysis.

The cause of this domain swapping is not immediately apparent, as the interactions between each C-terminal strand and the host molecule into which it is inserted are identical to those observed in the wild-type monomeric protein, so that there is no obvious energetic driving force for domain swapping. Furthermore, one would expect that tethering molecules into pairs in this manner should be accompanied by an entropic penalty. Some have suggested that domain swapping can be driven by geometric 'frustrations' at hinge regions (Ding *et al.*, 2006; Dehouck *et al.*, 2003). It is possible that the deletion

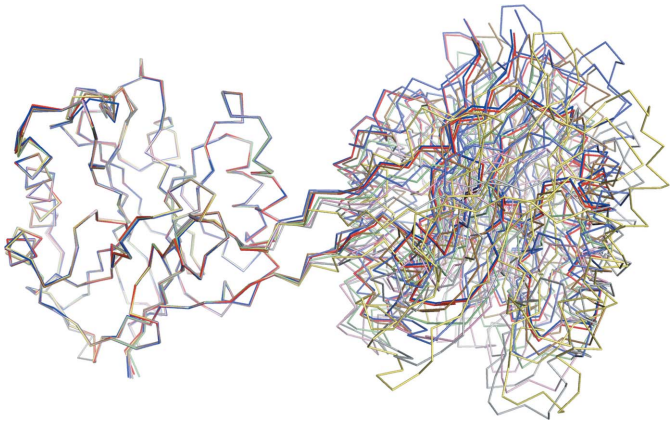

Figure 2
Superimposition of dimers by structural alignment with a single monomer reveals striking conformational heterogeneity arising from flexibility in the hinge region, although little difference is seen in the structures of the monomers themselves. The pairwise angles between lines traced along the hinge region from C^{α} of Thr266 to C^{α} of Trp272 differ by up to 40°. All molecules are shown as C^{α} traces.

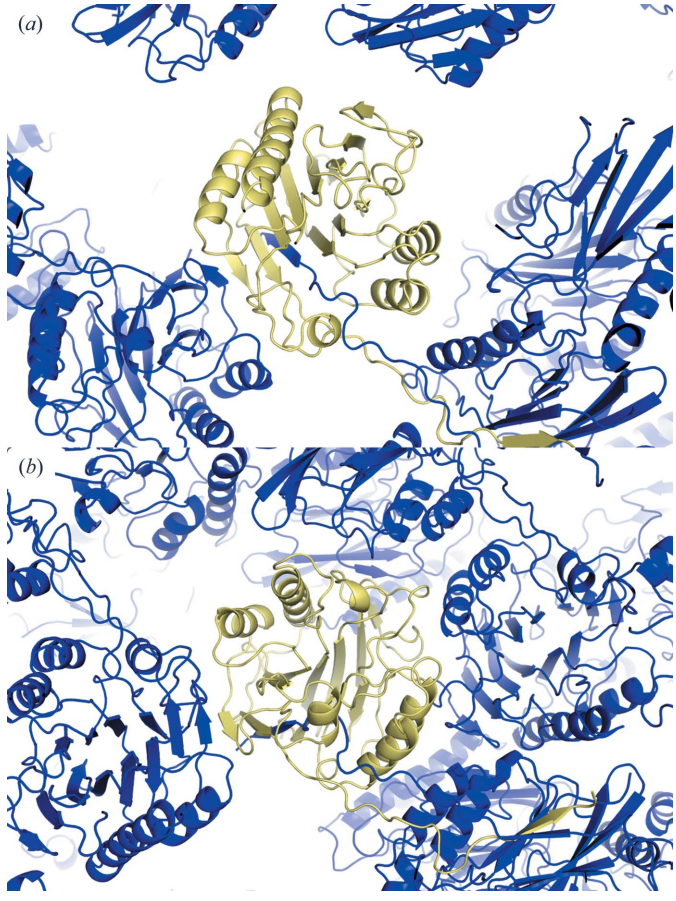

Figure 3
The environments of two monomers are quite different, accounting for the differences in *B* factors. (*a*) The monomer with the highest *B* factor (shown in pale yellow) interacts with its domain-swapping partner and is weakly associated with one other molecule through a short β-strand. (*b*) The monomer with the lowest *B* factor (also shown in pale yellow) interacts extensively with four other molecules including its domain-swapping partner and shows a weaker interaction through a short β-strand similar to that in (*a*).

of the β-hairpin makes the linking region between the β-strands immediately preceding and following the deletion site insufficiently flexible to accommodate the sharp turn required to maintain the topology of the wild-type protein. Domain swapping obviates the need for such a turn and may be energetically favored for this reason.

3.2. Conformational flexibility of dimers

Although each monomer in the asymmetric unit shows little structural deviation from the wild-type protein (with the exception of the swapped β-strand), superimposition of dimers reveals substantial conformational heterogeneity (Fig. 2), indicating that the hinge region acts not as a rigid link but rather as a flexible tether. It appears that the variation in the environment of each dimer imposed by the crystal lattice has caused a different relative orientation of monomer subunits to be preferred in each case, essentially trapping multiple conformational states in place. Smaller-scale conformational flexibility has been reported in other structures in which many distinct molecules are present within a single asymmetric unit (*e.g.* Winkler *et al.*, 1993; Muller *et al.*, 1997), but few structures exhibit such large-scale variation as that presented here, with monomers showing as much as a 40° difference in relative orientation when superimposed in the manner shown in Fig. 2.

Conformational flexibility was also shown by observed differences in thermal parameters among monomers. Owing to the low resolution, grouped isotropic *B*-factor refinement was performed, revealing substantial variation from one monomer to another. *B* factors averaged over whole chains ranged from 47 to 213 Å^2, with the latter case being significantly higher than for any other chain, most of which showed *B* factors around 100 Å^2. Inspection of the contacts made by the chain showing exceptionally high *B* factors reveals that it is involved in very limited contacts with other molecules and is thus held in place almost solely through its interaction with its domain-swapped partner (Fig. 3*a*). In contrast, the chains with lower *B* factors exhibit much more extensive contacts with other molecules (Fig. 3*b*), accounting for their decreased mobility.

The observed conformational flexibility is also likely to account for challenges in crystallization of the β-hairpin deletion mutant, which proved to be exceptionally recalcitrant in spite of the fact that other mutants and the wild-type protein are highly amenable to crystallographic study. The β-hairpin deletion mutant was crystallized only after extensive screening and optimization of crystallization conditions; of 35 crystals tested, only two showed diffraction beyond 4 Å resolution. Because the monomer structure is largely unchanged relative to that of wild-type β toxin, the intractability of the mutant probably solely arises from its flexibly linked dimeric form.

4. Summary and conclusions

Like other bacterial neutral sphingomyelinases, the staphylococcal hemolysin β toxin possesses a solvent-exposed hydrophobic β-hairpin which has been implicated in membrane adherence. Mutagenic deletion of this β-hairpin results in the unanticipated formation of domain-swapped dimers in which a C-terminal β-strand is exchanged between molecules. The cause of this domain swapping remains uncertain, but one likely possibility is that the bulky residues (Trp and Asn) flanking the deletion site cannot access the conformations required to form a short turn in order to maintain the topology of the wild-type enzyme. The exchanged β-strands instead form a flexible tether that links monomers together while still allowing substantial conformational freedom. Although this conformational flexibility hindered crystallographic study, it did not prevent successful determination of the structure of the mutant enzyme, which showed a multitude of distinct conformations trapped within a single crystal lattice. Remarkable heterogeneity in *B* factors was also indicative of molecular motion. Notably, those monomers that were engaged in extensive contacts with other molecules in the crystal showed *B* factors far lower than those of monomers that were in less restrictive environments. This structure represents both a unique example of domain swapping as an unintended consequence of mutagenesis and shows a broad sampling of conformational space by 16 crystallographically distinct enzyme monomers within a single asymmetric unit. A detailed discussion of the biological properties of this β-hairpin deletion mutant and several others is forthcoming.

Diffraction data were collected on the Advanced Photon Source beamline 14-BM-C. Computing facilities were provided by the Minnesota Supercomputing Institute Basic Sciences Computer Laboratory. We also thank Zu-Yi Gu for her excellent technical assistance.

References

Adams, P. D., Grosse-Kunstleve, R. W., Hung, L.-W., Ioerger, T. R., McCoy, A. J., Moriarty, N. W., Read, R. J., Sacchettini, J. C., Sauter, N. K. & Terwilliger, T. C. (2002). *Acta Cryst.* D**58**, 1948–1954.
Ago, H., Oda, M., Takahashi, M., Tsuge, H., Ochi, S., Katunuma, N., Miyano, M. & Sakurai, J. (2006). *J. Biol. Chem.* **281**, 16157–16167.
Bramley, A. J., Patel, A. H., O'Reilly, M., Foster, R. & Foster, T. J. (1989). *Infect. Immun.* **57**, 2489–2494.
Collins, J., Buckling, A. & Massey, R. C. (2008). *J. Clin. Microbiol.* **46**, 2112–2114.
Dehouck, Y., Biot, C., Gilis, D., Kwasigroch, J. M. & Rooman, M. (2003). *J. Mol. Biol.* **330**, 1215–1225.
Ding, F., Prutzman, K. C., Campbell, S. L. & Dokholyan, N. V. (2006). *Structure*, **14**, 5–14.
Dinges, M. M., Orwin, P. M. & Schlievert, P. M. (2000). *Clin. Microbiol. Rev.* **13**, 16–34.
Emsley, P. & Cowtan, K. (2004). *Acta Cryst.* D**60**, 2126–2132.
Hayashida, A., Bartlett, A. H., Foster, T. J. & Park, P. W. (2009). *Am. J. Pathol.* **174**, 509–518.
Huseby, M., Shi, K., Brown, C. K., Digre, J., Mengistu, F., Seo, K. S., Bohach, G. A., Schlievert, P. M., Ohlendorf, D. H. & Earhart, C. A. (2007). *J. Bacteriol.* **189**, 8719–8726.
Matthews, B. W. (1968). *J. Mol. Biol.* **33**, 491–497.
McCoy, A. J. (2007). *Acta Cryst.* D**63**, 32–41.
Mol, C. D., Kuo, C. F., Thayer, M. M., Cunningham, R. P. & Tainer, J. A. (1995). *Nature (London)*, **374**, 381–386.
Muller, Y. A., Christinger, H. W., Keyt, B. A. & de Vos, A. M. (1997). *Structure*, **5**, 1325–1338.
Oefner, C. & Suck, D. (1986). *J. Mol. Biol.* **192**, 605–632.
Openshaw, A. E., Race, P. R., Monzó, H. J., Vázquez-Boland, J. A. & Banfield, M. J. (2005). *J. Biol. Chem.* **280**, 35011–35017.
Otwinowski, Z. & Minor, W. (1997). *Methods Enzymol.* **276**, 307–326.
Painter, J. & Merritt, E. A. (2006). *Acta Cryst.* D**62**, 439–450.
Sambashivan, S., Liu, Y., Sawaya, M. R., Gingery, M. & Eisenberg, D. (2005). *Nature (London)*, **437**, 266–269.
Vagin, A. & Teplyakov, A. (1997). *J. Appl. Cryst.* **30**, 1022–1025.
Walev, I., Weller, U., Strauch, S., Foster, T. & Bhakdi, S. (1996). *Infect. Immun.* **64**, 2974–2979.
Winkler, F. K., Banner, D. W., Oefner, C., Tsernoglou, D., Brown, R. S., Heathman, S. P., Bryan, R. K., Martin, P. D., Petratos, K. & Wilson, K. S. (1993). *EMBO J.* **12**, 1781–1795.